COLOR BALANCE AND FUSION FOR UNDERWATER IMAGE ENHANCEMENT

Seminar Report

Submitted in partial fulfillment of the requirements for the award of degree of

BACHELOR OF TECHNOLOGY

In

COMPUTER SCIENCE AND ENGINEERING

of

APJ ABDUL KALAM TECHNOLOGICAL UNIVERSITY

Submitted By

ABHAY BALAN

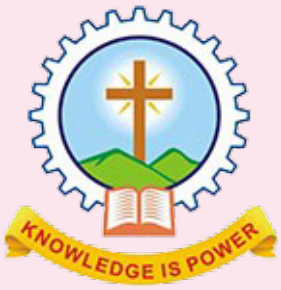

Department of Computer Science & Engineering
Mar Athanasius College Of Engineering Kothamangalam

COLOR BALANCE AND FUSION FOR UNDERWATER IMAGE ENHANCEMENT

Seminar Report

Submitted in partial fulfillment of the requirements for the award of degree of

BACHELOR OF TECHNOLOGY

In

COMPUTER SCIENCE AND ENGINEERING

of

APJ ABDUL KALAM TECHNOLOGICAL UNIVERSITY

Submitted By

ABHAY BALAN

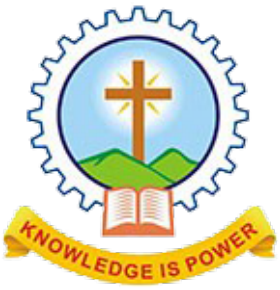

Department of Computer Science & Engineering
Mar Athanasius College Of Engineering Kothamangalam

DEPARTMENT OF COMPUTER SCIENCE AND ENGINEERING
MAR ATHANASIUS COLLEGE OF ENGINEERING
KOTHAMANGALAM

CERTIFICATE

This is to certify that the report entitled **Color Balance and Fusion for Underwater Image Enhancement** *submitted by* ***Mr.ABHAY BALAN****, Reg.No.* ***MAC15CS002*** *towards partial fulfillment of the requirement for the award of Degree of Bachelor of Technology in Computer science and Engineering from APJ Abdul Kalam Technological University for December 2018 is a bonafide record of the seminar carried out by him under our supervision and guidance.*

.....	.....	.....
Prof. Joby George	**Prof. Neethu Subash**	**Dr. Surekha Mariam Varghese**
Faculty Guide	***Faculty Guide***	***Head of the Department***

Date: Dept. Seal

ACKNOWLEDGEMENT

First and foremost, I sincerely thank the God Almighty for his grace for the successful and timely completion of the seminar.

I express my sincere gratitude and thanks to Dr. Solly George, Principal and Dr. Surekha Mariam Varghese, Head Of the Department for providing the necessary facilities and their encouragement and support.

I owe special thanks to the staff-in-charge Prof. Joby George, Prof.Neethu Subash and Prof Joby Anu Mathew for their corrections, suggestions and sincere efforts to co-ordinate the seminar under a tight schedule.

I express my sincere thanks to staff members in the Department of Computer Science and Engineering who have taken sincere efforts in helping me to conduct this seminar.

Finally, I would like to acknowledge the heartfelt efforts, comments, criticisms, co-operation and tremendous support given to me by my dear friends during the preparation of the seminar and also during the presentation without whose support this work would have been all the more difficult to accomplish.

ABSTRACT

Introduce an effective technique to enhance the images captured underwater and degraded due to the medium scattering and absorption. Our method is a single image approach that does not require specialized hardware or knowledge about the underwater conditions or scene structure. It builds on the blending of two images that are directly derived from a color- compensated and white-balanced version of the original degraded image. The two images to fusion, as well as their associated weight maps, are defined to promote the transfer of edges and color contrast to the output image. To avoid that the sharp weight map transitions create artifacts in the low frequency components of the reconstructed image, we also adapt a multiscale fusion strategy. Our extensive qualitative and quantitative evaluation reveals that our enhanced images and videos are characterized by better exposedness of the dark regions, improved global contrast, and edges sharpness. Our validation also proves that our algorithm is reasonably independent of the camera settings, and improves the accuracy of several image processing applications, such as image segmentation and key point matching.

Contents

List of Figures

LIST OF ABBREVIATION

UWLI	Underwater Lider imaging
DCP	Dark Channel Prior
UDCP	Underwater Dark Channel Prior
HR	High Resolution
HDR	High Dynamic Range
UDE	Underwater Depth Estimation

Introduction

Underwater environment offers many rare attractions such as marine animals and fishes, amazing landscape, and mysterious shipwrecks. Besides underwater photography, underwater imaging has also been an important source of interest in different branches of technology and scientific research , such as inspection of underwater infrastructures and cables , detection of man made objects , control of underwater vehicles , marine biology research , and archeology .

Different from common images, underwater images suffer from poor visibility resulting from the attenuation of the propagated light, mainly due to absorption and scattering effects. The absorption substantially reduces the light energy, while the scattering causes changes in the light propagation direction. They result in foggy appearance and contrast degradation,making distant objects misty. Practically, in common sea water images, the objects at a distance of more than 10 meters are almost unperceivable , and the colors are faded because their composing wavelengths are cut according to the water depth. There have been several attempts to restore and enhance the visibility of such degraded images. Since the deterioration of underwater scenes results from the combination of multiplicative and additive processes traditional enhancing techniques such as gamma correction, histogram equalization appear to be strongly limited for such a task. In the previous works that are surveyed , the problem has been tackled by tailored acquisition strategies using multiple images , specialized hardware or polarization filters . Despite of their valuable achievements, these strategies suffer from a number of issues that reduce their practical applicability.

In contrast, this paper introduces a novel approach to remove the haze in underwater images based on a single image captured with a conventional camera. Our approach builds on the fusion of multiple inputs, but derives the two inputs to combine by correcting the contrast and by sharpening a white-balanced version of a single native input image. The white balancing stage aims at removing the color cast induced by underwater light scattering, so as to produce a natural appearance of the sub-sea images. The multiscale implementation of the fusion process results in an artifact-free blending.

The rest of the paper is structured as follows. The next section briefly surveys the optical specificities of the under- water environment, before summarizing the work related to underwater dehazing. we present our novel white-balancing approach, especially designed for underwater images. Next section describes the main components of our fusion-based enhancing technique, including inputs and associated weight maps definition. Before concluding, we present comparative qualitative and quantitative assessments of our white-balancing and

fusion-based underwater dehazing techniques, as well as some results about their relevance to address common computer vision problems, namely image segmentation and feature matching.

Background knowledge

This section surveys the basic principles underlying light propagation in water.

For an ideal transmission medium the received light is influenced mainly by the properties of the target objects and the camera lens characteristics. This is not the case underwater. First, the amount of light available under water, depends on several factors. The interaction between the sun light and the sea surface is affected by the time of the day (which influences the light incidence angle), and by the shape of the interface between air and water (rough vs. calm sea). The diving location also directly impacts the available light, due to a location-specific color cast: deeper seas and oceans induce green and blue casts, tropical waters appear cyan, while protected reefs are characterized by high visibility. In addition to the variable amount of light available under water, the density of particles that the light has to go through is several hundreds of times denser in seawater than in normal atmosphere. As a consequence, sub-sea water absorbs gradually different wavelengths of light. Red, which corresponds to the longest wavelength, is the first to be absorbed (10-15 ft), followed by orange (20-25 ft), and yellow (35-45 ft). Pictures taken at 5 ft depth will have a noticeable loss of red. Furthermore, the refractive index of water makes judging distances difficult. As a result, underwater objects can appear 25 percentage larger than they really are.

The comprehensive studies of McGlamery[1] and Jaffe[2] have shown that the total irradiance incident on a generic point of the image plane has three main components in underwater mediums: direct component, forward scattering and back scattering. The direct component is the component of light reflected directly by the target object onto the image plane. At each image coordinate x the direct component is expressed as:

$$ED(x) = J(x)e^{n}d(x) = J(x)t(x) \qquad \text{(Equ: 1.1)}$$

J (x) is the radiance of the object
d(x) is the distance between the observer and the object, and
n is the attenuation coefficient
The exponential term **ed(x)** is also known as the transmission **t(x)**

Besides the absorption, the floating particles existing in the underwater mediums also

cause the deviation (scattering) of the incident rays of light. Forward-scattering results from a random deviation of a light ray on its way to the camera lens. It has been determined experimentally that its impact can be approximated by the convolution between the direct attenuated component, with a point spread function that depends on the distance between the image plane and the object. Back-scattering is due to the artificial light (e.g. flash) that hits the water particles, and is reflected back to the camera. Back-scattering acts like a glaring veil superimposed on the object. The influence of this component may be reduced significantly by simply changing the position and angle of the artificial light source so that most of the reflected particle light do not reach the camera. However, in many practical cases, back-scattering remains the principal source of contrast loss and color shifting in underwater images. Mathematically, it is often expressed as:

$$EBS(x) = B(x)(1 - e^n d(x)) \qquad \text{(Equ: 1.2)}$$

B(x)is a color vector known as the back-scattered light.
Ignoring the forward scattering component, the simplified underwater optical model thus becomes:

$$I(x) = J(x)e^n d(x) + B(x)(1 - e^n d(x)) \qquad \text{(Equ: 1.3)}$$

This simplified underwater camera model has a similar form than the model used to characterize the propagation of light in the atmosphere. It however does not reflect the fact that the attenuation coefficient strongly depends on the light wavelength, and thus the color, in underwater environments. Therefore, as discussed in the next section a straightforward extension of outdoor dehazing approaches performs poorly at great depth, in presence of non-uniform artificial illumination and selective absorption of colors. This is also why our approach does not resort to an explicit inversion of the light propagation model.

Related works

In this section, we will discuss various underwater image processing techniques used for recovery of distorted underwater images. The existing underwater dehazing techniques can be grouped in several classes. An important class corresponds to the methods using specialized hardware[3], second class consists in polarization-based method,third class of approaches employs multiple images or a rough approximation of the scene model.

2.1 WCID technique

A WCID means wavelength compensation and image dehazing. WCID is an underwater image enhancement method or technique which compensate wavelength. As discussed above, two main causes of underwater image distortions are light scattering and color change. Sometimes artificial light source is used to overcome insufficient lightening problem. But it introduce additional luminance in the image.WCID is an only technique which handles problems of light scattering, color change and artificial light source presence simultaneously. This technique has a novel systematic approach to enhance underwater images by dehazing algorithm . A number of underwater image processing techniques used to remove light scattering and color change effect. Generally most of the processing techniques focus on removing either light scattering effect or colour change effect. The only technique called WCID will handle these problems simultaneously . Fig 2.1 expline the image formation in WCID.

WCID is based on an underwater image formation model. the algorithm for wavelength compensation and image dehazing combines techniques to remove distortion caused by light scattering and color change .First ,Dark channel prior method is used to estimate distance between camera and object .based on the depth map derived ,the foreground and background areas are segmented .the light intensities of foreground and background are compared to determine presence of artificial light .if artificial light source is detected ,the luminance introduced by it is removed from the foreground area. Next dehazing algorithm is used to remove haze effect and color change.

2.2 Underwater lidar imaging system

Based on a newly-designed serial target, we firstly demonstrate the underwater LIDAR imaging in such a 3m short water tank with highly turbid waters successfully, and show the range-gated phenomenon in water much more clearly. The target-set comprises a series of

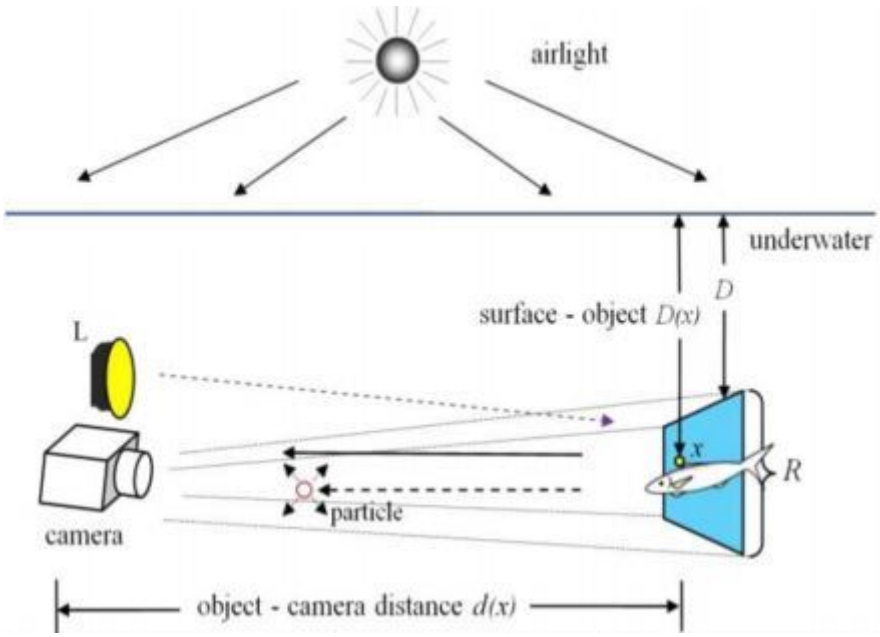

Fig. 2.1: image formation model

three bar test targets, which are set at intervals of 22.5cm roughly along the laser illumination direction since the light speed in water is 22.5 cm/ns.

We synchronize precisely the UWLI system[4] to range-gate on the targets which we want to capture their images, and to range-gate out the targets which we don't want their images. The attenuation coefficients in waters are 1.0/m and 2.3/m. Compared with non-gated case, the most distinct difference between the gates images and non-gated images in turbid water is that the nearer the target is located, the clearer its image is on the non-gated photos, but for the gated case the situation will be inverted completely when the delay time is adjusted suitably; that is, the image of the farther target could be much clearer than the image of the nearer target even in very turbid water.

2.3 Dark-channel prior method

A dark channel method is an efficient and effective method to restore original clarity of the underwater image. Images taken in the underwater environment are distorted because of light attenuation. Using ark channel prior ,the depth of the turbid water can be estimated by the assumption that most local patches in water free images contains some pixels which have very low intensities in at least one color channel. Dark channel prior is based on the statistics of clear images in air.

In pure water, it is very often that some pixels have very less intensity. Such pixels are known as dark pixels. In underwater images, the intensity of these dark pixels is contributed by background light. Therefore these dark pixels can directly provide accurate estimation of water transmission. Combining an underwater imaging model and a soft matting interpolation method, we can recover a high quality water free image and produce a good depth map .This approach is physically feasible and can obtain distant objects even in the heavy blur images. Dark channel prior may not be useful when scene object is inherently similar to the background light over a large local region and no shadow is cast on the object.

2.4 Histogram equalization

Histogram equalization is an image processing method which uses images histogram for image contrast adjustment. This method usually increases the contrast of distorted image by adjusting intensities. The method is useful in images with background and foregrounds that are both bright or both dark. Histogram equalization is a technique for adjusting image intensities to enhance contrast.Histogram equalization method cannot compensate light scattering problem. Fig 2.2 expline the histogram equlization applied to low contrast image.

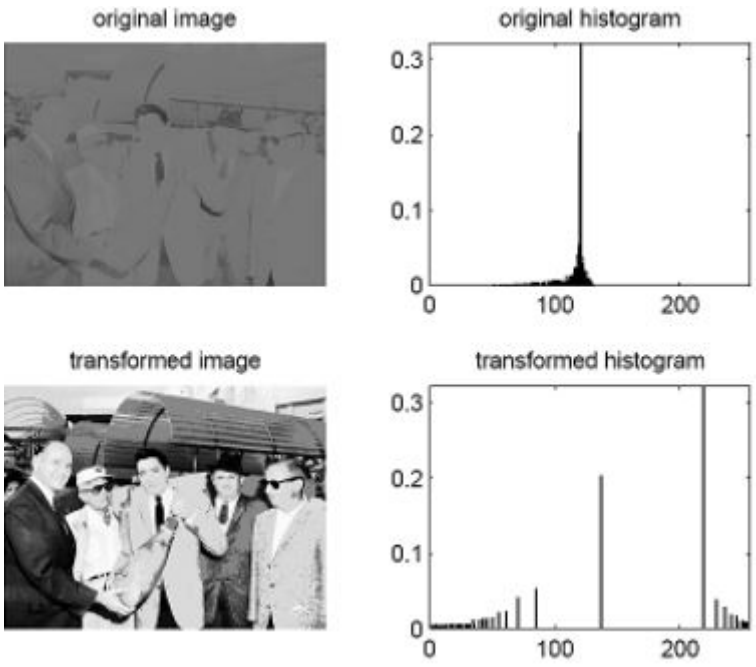

Fig. 2.2: histogram equalization applied to low contrast image

2.5 Deep photo system

introduce a novel system for browsing, enhancing, and manipulating casual outdoor photographs by combining them with already existing geo referenced digital terrain and urban models. A simple interactive registration process is used to align a photograph with such a model. Once the photograph and the model have been registered, an abundance of information, such as depth, texture, and GIS data, becomes immediately available to our system. This information, in turn, enables a variety of operations, ranging from dehazing and relighting the photograph, to novel view synthesis, and overlaying with geographic information. We describe the implementation of a number of these applications and discuss possible extensions. Our results show that augmenting photographs with already available 3D models of the world supports a wide variety of new ways for us to experience and interact with our everyday snapshots.

2.6 Image enhancement using an integrated colour model

proposed an approach based on slide stretching. The objective of this approach is twofold. Firstly, the contrast stretching of RGB algorithm is applied to equalize the colour contrast in images. Secondly, the saturation and intensity stretching of HSI is used to increase the true colour and solve the problem of lighting. Interactive software has been developed for underwater image enhancement.Flow chart fig 2.3 given below.

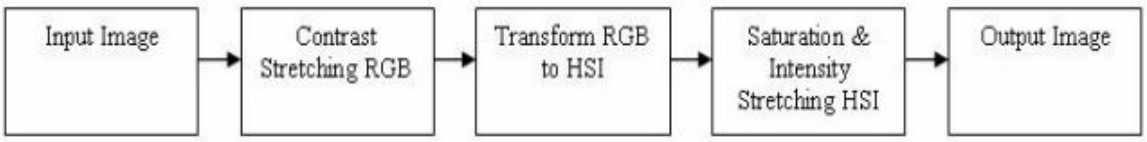

Fig. 2.3: flow Chart

When the contrast stretching algorithm is applied to colour images, each channel is stretched using the same scaling to maintain the correct colour ratio. The first step is to balance the red and green channel to be slightly the same to the blue channel. This is done by stretching the histogram into both sides to get well-spread histogram. In the second step we transform the RGB image into HSI, using the saturation and intensity transfer function to increase the true colour and brightness of underwater images. Using the transform function we have been able to stretch the saturation and intensity values of HSI colour model. Using the saturation parameters we can get the true colour of underwater images. Brightness of the colour is also considered to be important for underwater images. The HSI model also helps to solve the lighting problem using Intensity parameters.

The contrast stretching algorithm uses the linear scaling function to the pixel values. Each pixel is scaled using the following function :

$$Po = (Pic)x(bc)/(dc) + a \qquad \text{(Equ: 2.1)}$$

Po is the normalized pixel value
Pi is the considered pixel value
a is the minimum value of the desired range
b is the maximum value of the desired range
c is the lowest pixel value currently present in the image;
d is the highest pixel value currently present in the image.

Proposed method

Our image enhancement approach adopts a two step strategy, combining white balancing and image fusion, to improve underwater images without resorting to the explicit inversion of the optical model. In our approach, white balancing aims at compensating for the color cast caused by the selective absorption of colors with depth, while image fusion is considered to enhance the edges and details of the scene, to mitigate the loss of contrast resulting from back scattering.

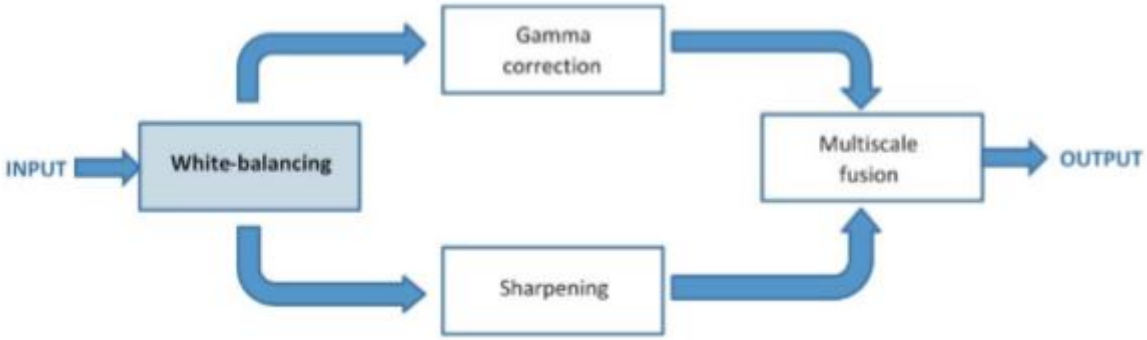

Fig. 3.1: proposed Method

3.1 Underwater white balance

White-balancing aims at improving the image aspect, primarily by removing the undesired color castings due to various illumination or medium attenuation properties. In underwater,the perception of color is highly correlated with the depth, and an important problem is the green-bluish appearance that needs to be rectied. As the light penetrates the water, the attenuation process affects selectively the wavelength spectrum, thus affecting the intensity and the appearance of a colored surface. Since the scattering attenuates more the long wavelengths than the short ones, the color perception is affected as we go down in deeper water. In practice, the attenuation and the loss of color also depends on the total distance between the observer and the scene.

We have considered the large spectrum of existing white balancing methods[5], and have identied a number of solutions that are both effective and suited to our problem (see Fig. 3.1).

In the following we briey revise those approaches and explain how they inspired us in the derivation of our novel approach proposed for underwater scenes.

Most of those methods make a specic assumption to estimate the color of the light source, and then achieve color constancy by dividing each color channel by its corresponding normalized light source intensity. Among those methods, the Gray world algorithm assumes that the average reectance in the scene is achromatic. Hence, the illuminant color distribution is simply estimated by averaging each channel independently. The Max RGB assumes that the maximum response in each channel is caused by a white patch, and consequently estimates the color of the light source by employing the maximum response of the different color channels. In their Shades-of-Grey method , Finlayson etal rst observe that Max-RGB and Gray-World are two instantiations of the Minkowski p-norm applied to the native pixels, respectively with p = 0 and p = 1, and propose to extend the process to arbitrary p values. The best results are obtained for p = 6. The Grey-Edge hypothesis of van de Weijer et al. further extends this Minkowski norm framework. It assumes the average edge difference in a scene to be achromatic, and computes the scene illumination color by applying the Minkowski p-norm on the derivative structure of image channels, and not on the zero-order pixel structure, as done in Shades of Grey.

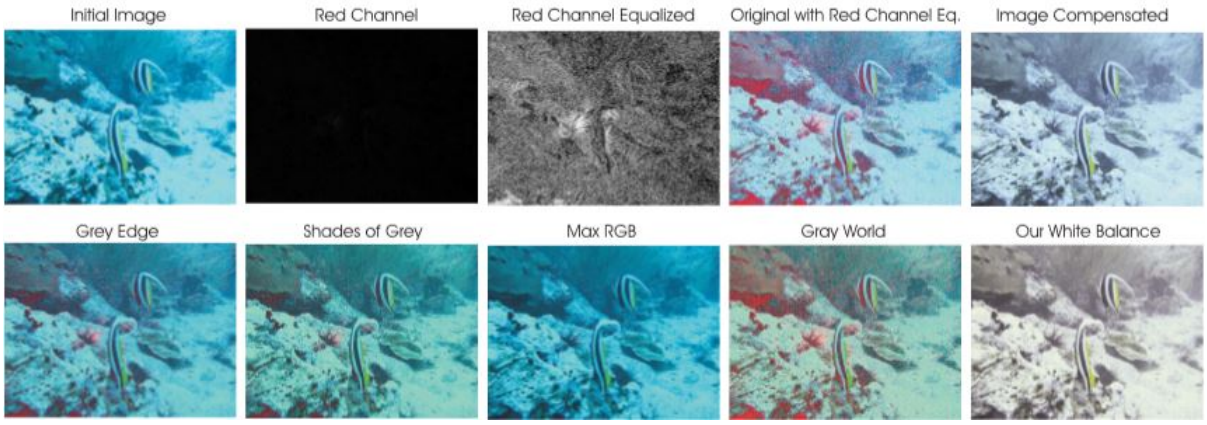

Fig. 3.2: Underwater white-balancing
Top row from left to right: initial underwater image with highly attenuated red channel, original red channel and red channel after histogram equalization, original image with the red channel equalized and the image after employing our compensation expressed by Eq.4. The image compensated is obtained by simply replacing the compensated red channel Eq.4 in the original underwater image. Bottom row from left to right: several well-known white balancing approaches (Gray Edge , Shades of Gray , Gray World[6] and Max RGB[7]). Please notice the artifacts (red colored locations) that appear due to the lack of information on the red channel.

Despite of its computational simplicity, this approach has been shown to obtain comparable results than state-of-the-art color constancy methods, such as the recent method of that

relies on natural image statistics.

When focusing on underwater scenes, we have found through the comprehensive study presented in Fig. 3.3 and Table I that the well-known Gray-World algorithm achieves good visual performance for reasonably distorted underwater scenes. However, a deeper investigation dealing with extremely deteriorated underwater scenes (see Fig. 3.2) reveals that most traditional methods perform poorly. They fail to remove the color shift, and generally look bluish. The methods that best remove the bluish tone is the Grey World, but we observe that this method suffers from severe red artifacts. Those artifacts are due to a very small mean value for the red channel, leading to an overcompensation of this channel in locations where red is present (because Gray world divides each channel by its mean value). To circumvent this issue, following the conclusions of previous underwater works, we therefore primarily aim to compensate for the loss of the red channel. In a second step, the Gray World algorithm will be adopted to compute the white balanced image.

To compensate for the loss of red channel, we build on the four following observations/principles:

1. The green channel is relatively well preserved under water, compared to the red and blue ones. Light with a long wavelength, i.e. the red light, is indeed lost rst when traveling in clear water;

2. The green channel is the one that contains opponent color information compared to the red channel, and it is thus especially important to compensate for the stronger attenuation induced on red, compared to green. Therefore, we compensate the red attenuation by adding a fraction of the green channel to red. We had initially tried to add both a fraction of green and blue to the red but, as can be observed in Fig. 3.3, using only the information of the green channel allows to better recover the entire color spectrum while maintaining a natural appearance of the background (water regions);

3. The compensation should be proportional to the difference between the mean green and the mean red values because, under the Gray world assumption (all channels have the same mean value before attenuation), this difference reects the disparity/unbalance between red and green attenuation;

4. To avoid saturation of the red channel during the Gry World step that follows the red loss compensation, the enhancement of red should primarily affect the pixels with small red channel values, and should not change pixels that already include a signicant red component. In other words, the green channel information should not be transferred in regions where the information of the red channel is still signicant. Thereby, we want to avoid the reddish appearance introduced by the Gray-World algorithm in the over-exposed regions (see Fig. 3.2). Basically,

the compensation of the red channel has to be performed only in those regions that are highly attenuated (see Fig. 3.1). This argument follows the statement in , telling that if a pixel has a signicant value for the three channels, this is because it lies in a location near the observer, or in an articially illuminated area, and does not need to be restored.

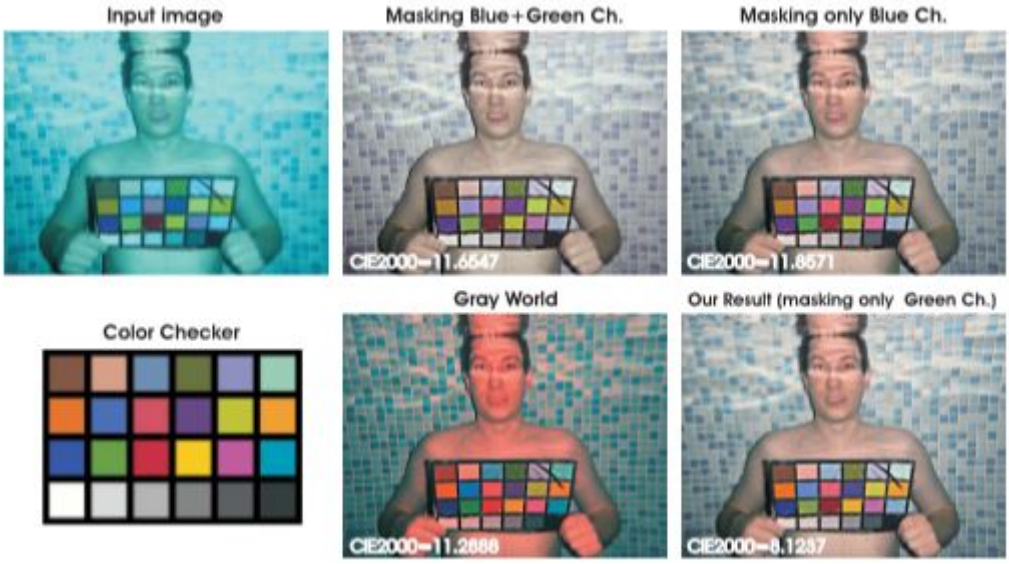

Fig. 3.3: Compensating the red channel

Since for underwater scenes the blue channel contains most of the details, using this information will reduce the ability to recover certain colors such as yellow and orange and also it tends to transform the blue areas to violet shades. Compensating the red channel by masking only the green channel (Equation (4)) these limitations are reduced signicantly. This is conrmed visually but also by computing the CIE2000 measure using as a reference the color checker (displayed with white ink on the resulted images.

Mathematically, to account for the above observations, we propose to express the compensated red channel Irc at every pixel location (x) as follows:

$$Irc(x) = Ir(x) + a.(Igm - Irm).(1 - Ir(x)).Ig(x), \qquad \text{(Equ: 3.1)}$$

Ir Red color channels of image I

Ig green color channels of image I (each channel being in the interval [0, 1])

Irm mean value of Ir

Igm mean value of Ig

a denotes a constant parameter.

In Equation 3.1, each factor in the second term directly results from one of the above observa-

tions, and a denotes a constant parameter. In practice, our tests have revealed that a value of a=1 is appropriate for various illumination conditions and acquisition settings.

To complete our discussion about the severe and color dependent attenuation of light under water, it is worth noting the works in which reveal and exploit the fact that, in turbid waters or in places with high concentration of plankton, the blue channel may be signicantly attenuated due to absorption by organic matter. To address those cases, when blue is strongly attenuated and the compensation of the red channel appears to be insufcient, we propose to also compensate for the blue channel attenuation, i.e. we compute the compensated blue channel Ibc as:

$$Ibc(x) = Ib(x) + a.(Igm - Ibm).(1 - Ib(x)).Ig(x) \quad \text{(Equ: 3.2)}$$

Ib Red color channels of image I
Ig green color channels of image I (each channel being in the interval [0, 1])
Ibm mean value of Ir
Igm mean value of Ig
a denotes a constant parameter.

where Ib, Ig represent the blue and green color channels of image I, and is also set to one. In the rest of the paper, the blue compensation is only considered. All other results are derived based on the sole red compensation. After the red (and optionally the blue) channel attenuation has been compensated, we resort to the conventional Gray-World assumption to estimate and compensate the illuminant color cast.

shown in Fig. 3.4, our white-balancing approach reduces the quantization artifacts introduced by domain stretching (the red regions in the different outputs). The reddish appearance of high intensity regions is also well corrected since the red channel is better balanced. As will be extensively discussed in Section V-A, our approach shows the highest robustness compared to the other well-known white-balancing techniques. In particular, whilst being conceptually simplest, we observe in Fig. 3.5 that, in cases for which the red channel of the underwater image is highly attenuated, it outperforms the white balancing strategy introduced in our conference version of our fusion-based underwater dehazing method[8] .

Additionally, Fig. 3.4 shows that using our white balancing strategy yields signicant improvement in estimating transmission based on the well-known DCP. As can be seen in the rst seven columns of Fig. 3.4, estimating the transmission maps based on DCP, using the initial

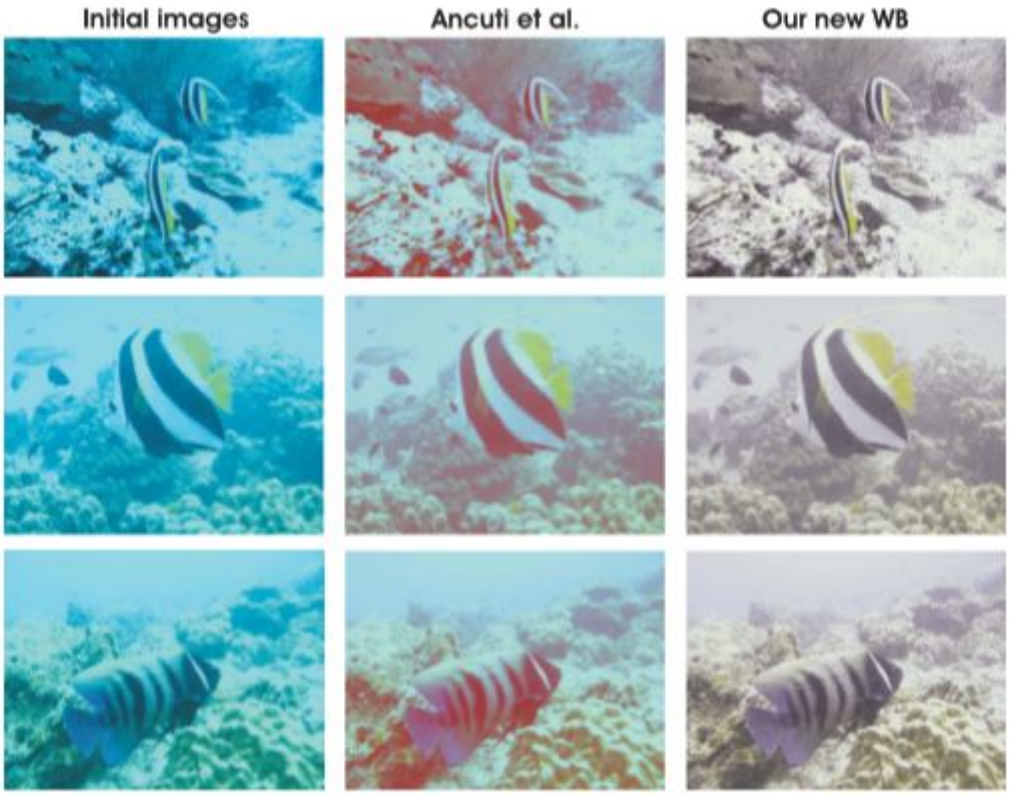

Fig. 3.4: Comparison to our previous white balancing approach .

underwater images but also the processed versions with several well-known white balancing approaches (Gray Edge , Shades of Gray , Max RGB and Gray World) yields poor estimates. In contrast, by simply applying DCP on our white balanced image version we obtain comparable and even better estimates than the specialized underwater techniques of UDCP[9] , MDCP[10] and BP .

Despite white balancing is crucial to recover the color, using this correction step is not sufcient to solve the dehazing problem since the edges and details of the scene have been affected by the scattering. In the next section, we therefore propose an effective fusion based approach, relying on gamma correction and sharpening to deal with the hazy nature of the white balanced image.

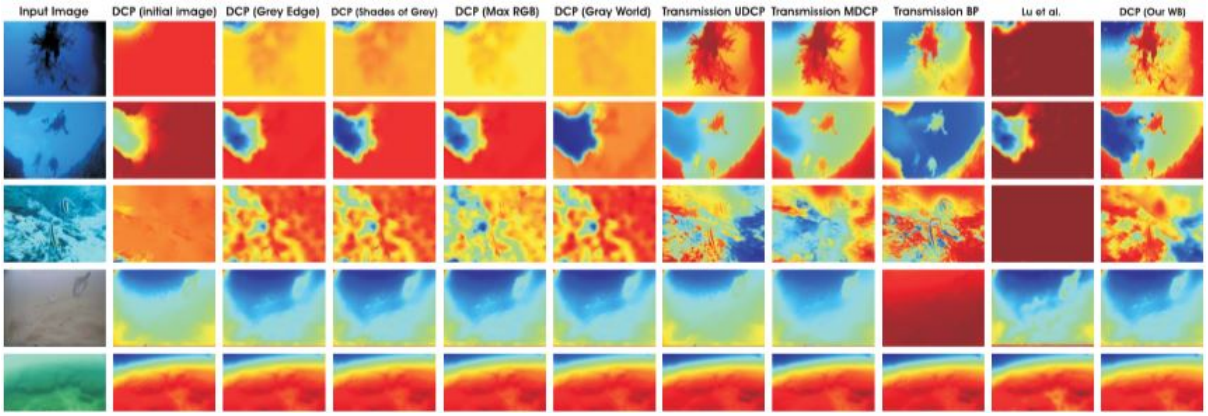

Fig. 3.5: Comparison to our previous white balancing approach
Underwater transmission estimation. Columns 2 to 6, the transmission map is estimated based on DCP applied to the initial underwater images but also from versions obtained with several well-known white balancing approaches (Gray Edge , Shades of Gray , Max RGB and Gray World) yield poor estimates. In contrast, applying DCP on our white balanced image version (last column), results in comparable and even better estimates compared with the specialized underwater techniques corresponding to UDCP, MDCP , BP and Lu et al.

3.2 Multi-scale fusion

In this work we built on the multi-scale fusion principles to propose a single image underwater dehazing solution. Image fusion has shown utility in several applications such as image compositing , multi spectral video enhancement , defogging and HDR imaging. Here, we aim for a simple and fast approach that is able to increase the scene visibility in a wide range of underwater videos and images.Our framework builds on a set of inputs and weight maps derived from a single original image.However, those ones are specically chosen in order to take the best out of the white-balancing method introduced in the previous section. In particular, as depicted in Fig 3.1, a pair of inputs is introduced to respectively enhance the color contrast and the edge sharpness of the white-balanced image, and the weight maps are dened to preserve the qualities and reject the defaults of those inputs, i.e. to overcome the artifacts induced by the light propagation limitation in underwater medium.

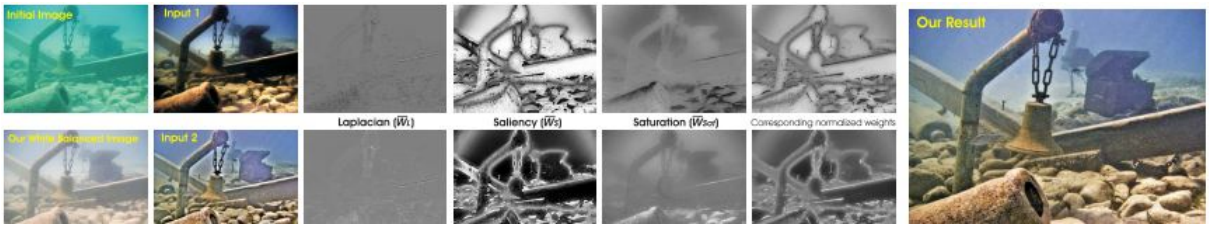

Fig. 3.6: The two inputs derived from our white balanced image version
The three corresponding normalized weight maps for each of them, the corresponding normalized weight maps and our nal result.

This multi-scale fusion signicantly differs from our previous fusion-based underwater dehazing approach published at IEEE CVPR . To derive the inputs from the original image, our initial CVPR algorithm did assume that the backscattering component (due to the articial light that hits the water particles and is then reected back to the camera) has a reduced inuence. This assumption is generally valid for underwater scenes decently illuminated by natural light, but fails in more challenging illumination scenarios. In contrast,this paper does not rely on the optical model and proposes an alternative denition of inputs and weights to deal with severely degradaded scenes. As depicted in Fig. 3.7 and detailed below, our underwater dehazing technique consists in three main steps: inputs derivation from the white balanced underwater image, weight maps denition, and multi-scale fusion of the inputs and weight maps.

3.2.1 Inputs for fusion process

Since the color correction is critical in underwater, we rst apply our white balancing technique to the original image. This step aims at enhancing the image appearance by discarding unwanted color casts caused by various illuminants. In water deeper than 30 ft, white balancing suffers from noticeable effects since the absorbed colors are difcult to be recovered. As a result, to obtain our rst input we perform a gamma correction of the white balanced image version. Gamma correction aims at correcting the global contrast and is relevant since, in general, white balanced underwater images tend to appear too bright. This correction increases the difference between darker/lighter regions at the cost of a loss of details in the under-/over-exposed regions. To compensate for this loss, we derive a second input that corresponds to a sharpened version of the white balanced image. Therefore, we follow the unsharp masking principle,in the sense that we blend a blurred or unsharp (here Gaussian ltered) version of the image with the image to sharpen. The typical formula for unsharp masking denes the sharpened image S as:

$$S = I + b(I - G * I), \qquad \text{(Equ: 3.3)}$$

I is the image to sharpen (in our case the white balanced image)
G * I denotes the Gaussian ltered version of I
b is a parameter

In practice, the selection of **b** is not trivial. A small **b** fails to sharpen I, but a too large **b** results in over-saturated regions, with brighter highlights and darker shadows. To circumvent this problem, we dene the sharpened image S as follows:

$$S = (I + N(I - G * I))/2 \qquad \text{(Equ: 3.4)}$$

N. denoting the linear normalization operator (histogram stretching).
This operator shifts and scales all the color pixel intensities of an image with a unique shifting and scaling factor dened so that the set of transformed pixel values cover the entire available dynamic range. The sharpening method dened in 3.6 is referred to as normalized unsharp masking process in the following. It has the advantage to not require any parameter tuning, and appears to be effective in terms of sharpening. This second input primarily helps in reducing the degradation caused by scattering. Since the difference between white balanced image and its Gaussian ltered version is a high pass signal that approximates the opposite of Laplacian, this operation has the inconvenient to magnify the high frequency noise, thereby generating

undesired artifacts in the second input . The multi-scale fusion strategy described in the next section will be in charge of minimizing the transfer of those artifacts to the nal blended image.

3.2.2 Weights of the fusion process

The weight maps are used during blending in such a way that pixels with a high weight value are more represented in the nal image (see Fig 3.6). They are thus dened based on a number of local image quality or saliency metrics.

Laplacian contrast weight (WL) estimates the global contrast by computing the absolute value of a Laplacian lter applied on each input luminance channel. This straightforward indicator was used in different applications such as tone mapping and extending depth of eld since it assigns high values to edges and texture. For the underwater dehazing task, however, this weight is not sufcient to recover the contrast, mainly because it can not distinguish much between a ramp and at regions. To handle this problem, we introduce an additional and complementary contrast assessment metric.

Saliency weight (WS) aims at emphasizing the salient objects that lose their prominence in the underwater scene. To measure the saliency level, we have employed the saliency estimator of Achantay et al. This computationally efcient algorithm has been inspired by the biological concept of center-surround contrast. However, the saliency map tends to favor highlighted areas (regions with high luminance values). To overcome this limitation, we introduce an additional weight map based on the observation that saturation decreases in the highlighted regions.

Saturation weight (WSat) enables the fusion algorithm to adapt to chromatic information by advantaging highly saturated regions. This weight map is simply computed (for each input Ik) as the deviation (for every pixel location) between the Rk,Gk and Bk color channels and the luminance Lk of the kth input:

$$WSat = \sqrt{1/3[(Rk - Lk)^2 + (Gk - Lk)^2 + (Bk - Lk)^2]} \qquad \text{(Equ: 3.5)}$$

In practice,for each input,the three weight maps are merged in a single weight map as follows. For each input k, an aggregated weight map Wk is rst obtained by summing up the three WL, WS, and WSat weight maps. The K aggregated maps are then normalized on a pixel-per-pixel basis, by dividing the weight of each pixel in each map by the sum of the weights of the same pixel over all maps. The normalized weights of corresponding weights are shown at the bottom of Fig. 3.5 Note that, in comparison with our previous work , we limit

ourselves to these three weight maps only, and we do not compute the exposedness weight map anymore.

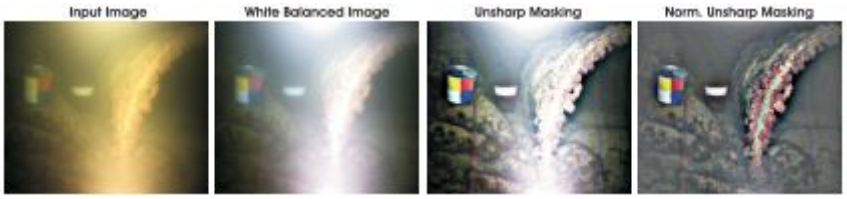

Fig. 3.7: Comparison between traditional unsharp masking and normalized unsharp masking applied on the white balanced image.

In addition to reducing the overall complexity of the fusion process, we have observed that, when using the two inputs proposed in this paper, the exposedness weight map tends to amplify some artifacts, such as ramp edges of our second input, and to reduce the benet derived from the gamma corrected image in terms of image contrast. We explain this observation as follows. Originally, in an exposure fusion context , the exposedness weight map had been introduced to reduce the weight of pixels that are under- or over-exposed. Hence, this weight map assigns large (small) weight to input pixels that are close to (far from) the middle of the image dynamic range. In our case, since the gamma corrected input tends to exploit the whole dynamic range, the use of the exposedness weight map tends to penalize it in favor of the sharpened image, thereby inducing some sharpening artifacts and missing some contrast enhancements.

3.2.3 Naive fusion process

Given the normalized weight maps, the reconstructed image R(x) could typically be obtained by fusing the dened inputs with the weight measures at every pixel location (x):

$$R(x) = \sum_{k=1}^{k} Wk(x)Ik(x) \qquad \text{(Equ: 3.6)}$$

Ik denotes the input (k is the index of the inputs K = 2 in our case).

wk denotes the normalized weight map

In practice, the naive approach introduces undesirable halos . A common solution to overcome this limitation is to employ multi-scale linear or non-linear lters.

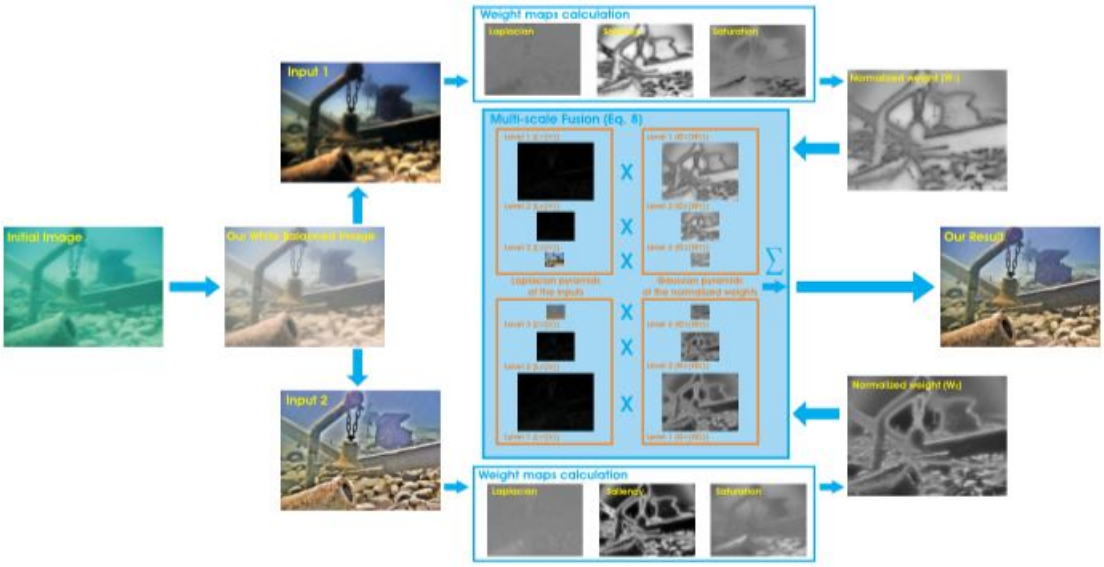

Fig. 3.8: Overview of our dehazing scheme.

Two images, denoted Input 1 and Input 2, are derived from the (too pale) white balanced image, using Gamma correction and edge sharpening, respectively. Those two images are then used as inputs of the fusion process, which derives normalized weight maps and blends the inputs based on a multi-scale process. The multi-scale fusion approach is here exemplied with only three levels of the Laplacian and Gaussian pyramids.

3.2.4 Multi-scale fusion process

The multi-scale decomposition is based on Laplacian pyramid originally described in Burt and Adelson . The pyramid representation decomposes an image into a sum of bandpass images. In practice, each level of the pyramid does lter the input image using a low-pass Gaussian kernel G, and decimates the ltered image by a factor of 2 in both directions. It then subtracts from the input an up-sampled version of the low-pass image, thereby approximating the (inverse of the) Laplacian, and uses the decimated low-pass image as the input for the subsequent level of the pyramid. Formally, using Gl to denote a sequence of l low-pass ltering and decimation, followed by l up-sampling operations, we dene the N levels Ll of the pyramid as follows:

$$I(x) = \sum_{l=1}^{N} Ll[I(x)] \qquad \text{(Equ: 3.7)}$$

Ll represent the lth level of the Laplacian pyramid

To write the equation, all those images have been up-sampled to the original image dimension. However, in an efcient implementation, each level l of the pyramid is manipulated at native subsampled resolution. Following the traditional multi-scale fusion strategy , each source input Ik is decomposed into a Laplacian pyramid while the normalized weight maps Wk are decomposed using a Gaussian pyramid. Both pyramids have the same number of levels, and the mixing of the Laplan the image size, and has a direct impact on the visual quality of the blended image. The dehazed output is obtained by summing the fused contribution of all levels, after appropriate upsampling. By independently employing a fusion process at every scale level, the potential artifacts due to the sharp transitions of the weight maps are minimized.fig 3.8 represent the all steps in our proposed system. Multi-scale fusion is motivated by the human visual system, which is very sensitive to sharp transitions appearing in smooth image patterns, while being much less sensitive to variations/artifacts occurring on edges and textures (masking phenomenon). Interestingly, a recent work has shown that the multiscale process can be approximated by a computationally efcient and visually pleasant single-scale procedure . This single scale approximation should denitely be encouraged when cian inputs with the Gaussian normalized weights is performed independently at each level l:

$$I(x) = \sum_{l=1}^{K} Gl[Wk(x)] * Ll[I(x)] \qquad \text{(Equ: 3.8)}$$

l denotes the pyramid levels
K refers to the number of input images
Gl represent the lth level of the Gussian pyramid
Ll represent the lth level of the Laplacian pyramid
N Number of level(Depends)

where l denotes the pyramid levels and k refers to the number of input images. In practice, the number of levels N depend on the image size, and has a direct impact on the visual quality of the blended image. The dehazed output is obtained by summing the fused contribution of

all levels, after appropriate by up sampling independently employing a fusion process at every scale level, the potential artifacts due to the sharp transitions of the weight maps are minimized. Multi-scale fusion is motivated by the human visual system, which is very sensitive to sharp transitions appearing in smooth image patterns, while being much less sensitive to variation-s/artifacts occurring on edges and textures (masking phenomenon). Interestingly, a recent work has shown that the multiscale process can be approximated by a computationally efcient and visually pleasant single-scale procedure. This single scale approximation should denitely be encouraged when complexity is an issue, since it also turns the multi resolution process into a spatially localized procedure.

	Grey-Edge		**Shades of Grey**		**max-RGB**		**Grey-World**		**Ancuti et al.**		**Our WB**	
	CIE2000	Q_u	CIE2000	Q_u	CIE2000	Q_u	CIE2000	Q_u	CIE2000	Q_u	CIE2000	Q_u
Cannon D10	14.8368	0.5810	9.1694	0.6185	12.8245	0.5737	9.9290	0.6435	9.4534	0.6321	9.4055	0.6303
FujiFilm Z33	18.8104	0.5798	9.2788	0.7394	15.4398	0.6384	9.3965	0.7601	10.7183	0.6874	12.7031	0.6599
Olympus T6000	17.4335	0.6092	9.5245	0.6568	14.6394	0.6136	11.7903	0.6966	10.2549	0.6805	8.4598	0.7164
Olympus T8000	18.5834	0.5947	13.5059	0.6844	17.4925	0.6195	14.4812	0.6396	11.7469	0.7023	8.9903	0.7128
Panasonic TS1	12.8787	0.6501	12.9742	0.6672	15.3450	0.6756	13.3113	0.6419	12.9008	0.6814	8.9686	0.6858
Pentax W60	13.1949	0.5573	7.6364	0.6317	9.7164	0.5634	9.8853	0.7009	7.7004	0.6497	8.9194	0.6447
Pentax W80	12.9933	0.6816	8.3278	0.7510	10.7710	0.6816	8.7854	0.6993	8.3631	0.7263	7.2347	0.7652
Average	15.5330	0.6077	10.0596	0.6784	13.7469	0.6237	11.0827	0.6831	10.1625	0.6801	9.2402	0.6879

Fig. 3.9: White balancing quantitative evaluvation based on CIEDE 2000 and Qunmeasure

Fig. 3.10: Comparative results of different white balancing techniques.
From left to right: 1. Original underwater images taken with different cameras; 2. Gray Edge ; 3. Shades of Gray ; 4. Max RGB ; 5. Gray World ; 6. Our previous white balancing technique 7. Our new white balancing technique. The cameras used to take the pictures are Canon D10, FujiFilm Z33, Olympus Tough 6000, Olympus Tough 8000, Pentax W60, Pentax W80, Panasonic TS1

Conclusion

We have presented an alternative approach to enhance underwater videos and images. Our strategy builds on the fusion principle and does not require additional information than the single original image. We have shown in our experiments that our approach is able to enhance a wide range of underwater images (e.g. different cameras, depths, light conditions)with high accuracy,being able to recover important faded features and edges. Moreover, for the rst time, we demonstrate the utility and relevance of the proposed image enhancement technique for several challenging underwater computer vision applications.

REFERENCES

[1] M. D. Kocak, F. R. Dalgleish, M. F. Caimi, and Y. Y. Schechner, A focus on recent developments and trends in underwater imaging, Marine Technol. Soc. J., vol. 42, no. 1, pp. 5267, 2008.

[2] Y. Y. Schechner and Y. Averbuch, Regularized image recovery in scattering media, IEEE Trans. Pattern Anal. Mach. Intell., vol. 29, no. 9, pp. 16551660, Sep. 2007.

[3] B. L. McGlamery, A computer model for underwater camera systems, Proc. SPIE, vol. 208, pp. 221231, Oct. 1979.

[4] Y. Y. Schechner and Y. Averbuch, Regularized image recovery in scattering media, IEEE Trans. Pattern Anal. Mach. Intell., vol. 29, no. 9, pp. 16551660, Sep. 2007

[5] M. Ebner, Color Constancy, 1st ed. Hoboken, NJ, USA: Wiley, 2007.

[6] G. Buchsbaum, A spatial processor model for object colour perception, J. Franklin Inst., vol. 310, no. 1, pp. 126, Jul. 1980.

[7] E. H. Land, The Retinex theory of color vision, Sci. Amer., vol. 237, no. 6, pp. 108128, Dec. 1977.

[8] C. Ancuti, C. O. Ancuti, T. Haber, and P. Bekaert, Enhancing underwater images and videos by fusion, in Proc. IEEE CVPR, Jun. 2012, pp. 8188.

[9] P. L. J. Drews, Jr., E. R. Nascimento, S. S. C. Botelho, and M. F. M. Campos, Underwater depth estimation and image restoration based on single images, IEEE Comput. Graph. Appl., vol. 36, no. 2, pp. 2435, Mar./Apr. 2016.

[10] K. B. Gibson, D. T. Vo, and T. Q. Nguyen, An investigation of dehazing effects on image and video coding, IEEETrans. Image Process., vol. 21, no. 2, pp. 662673, Feb. 2012.